Madhania, Suci; Muharam, Yuswan; Winardi, Sugeng; Purwanto, Widodo Wahyu

Article

Mechanism of molasses-water mixing behavior in bioethanol fermenter: Experiments and CFD modeling

Energy Reports

Provided in Cooperation with:
Elsevier

Suggested Citation: Madhania, Suci; Muharam, Yuswan; Winardi, Sugeng; Purwanto, Widodo Wahyu (2019) : Mechanism of molasses-water mixing behavior in bioethanol fermenter: Experiments and CFD modeling, Energy Reports, ISSN 2352-4847, Elsevier, Amsterdam, Vol. 5, pp. 454-461, https://doi.org/10.1016/j.egyr.2019.04.008

This Version is available at:
https://hdl.handle.net/10419/243600

Energy Reports 5 (2019) 454–461

Contents lists available at ScienceDirect

Energy Reports

journal homepage: www.elsevier.com/locate/egyr

Research paper

Mechanism of molasses–water mixing behavior in bioethanol fermenter. Experiments and CFD modeling

Suci Madhania [a,b], Yuswan Muharam [a], Sugeng Winardi [b], Widodo Wahyu Purwanto [a,*]

[a] Department of Chemical Engineering, Faculty of Engineering, Universitas Indonesia, Depok, Indonesia
[b] Department of Chemical Engineering, Institut Teknologi Sepuluh Nopember, Surabaya, Indonesia

HIGHLIGHTS

- Experiments and CFD modeling of molasses–water mixing behavior in a stirred-tank.
- The rheological characterization molasses is a non-Newtonian fluid exhibits shear thinning behavior.
- Combined Eulerian-LES model is the closest to the experimental results.

ARTICLE INFO

Article history:
Received 28 September 2018
Received in revised form 15 April 2019
Accepted 16 April 2019
Available online xxxx

Keywords:
Bioethanol
Computational fluid dynamics
Mixing behavior
Molasses–water
Rheology
Stirred-tank

ABSTRACT

Molasses is a first-generation bioethanol feedstock that is a byproduct of sugar production. Molasses is a viscous fluid; consequently, when it serves as a substrate, it needs to be dissolved in water to obtain the appropriate conditions for the yeast. Therefore, the mixing process of molasses and water is an essential factor that significantly affects the efficiency of the fermentation process. This work aims to study the molasses–water mixing behavior in a cylindrical cone-shaped stirred-tank system reviewed by the effect of the molasses–water rheological characteristics. The molasses–water mixing behavior was investigated through a simple visualization method by using a camera and a 650 nm red laser as an observation plane of molasses–water interface height changes. Based on the results of the rheological characterization, it is known that molasses are a non-Newtonian fluid that exhibits shear thinning behavior. A rheological model molasses–water mixture has been developed. The behavior of molasses–water mixture comprises three zone mechanisms. The Eulerian multiphase model is the closest to the experimental results, and the combination of the Eulerian multiphase model and Large Eddy Simulation can be applied to predict the mixing behavior in an industrial scale stirred-tank.

1. Introduction

Fossil-fuel-based energy sources are being increasingly depleted, encouraging the efforts to fulfill the need for energy by using alternative energy sources. Bioethanol (C_2H_5OH) is one of the alternative energy sources that is derived from plants and can function as a substitute fuel. The use of bioethanol as a substitute is expected to minimize the use of fossil fuels and reduce CO_2 emissions. Bioethanol can be produced through the fermentation process by using raw materials such as sucrose-containing materials (e.g., sugarcane de Carvalho et al., 2016, sugar beet and fruits), starch materials (e.g., cassava, corn Chao et al., 2017, sweet potatoes Virgínio e Silva et al., 2017), lignocellulosic materials (grass (Liu et al., 2017), waste paper (Wang et al., 2012; Byadgi and Kalburgi, 2016), corncob (Boonchuay et al., 2018), and wheat straw (Tomás-Pejó et al., 2009) and algae (Khambhaty et al., 2012; Bibi et al., 2017)

Much effort has been made to increase the production yield of bioethanol, such as process optimization of distillation (Tgarguifa et al., 2017) and increasing the efficiency of fermentation by using immobilized yeast (Mohd Azhar et al., 2017). Stirring of the raw materials is expected to improve the efficiency of fermentation. Optimal mixing causes the yeast to be evenly distributed in the fermenter so that the contact between the yeast and the broth is maximum, which renders the fermentation reaction efficient. Computational investigations are more efficient and economical for studying the influence of the mixing process in an industrial-scale system. However, for implementation, some information is needed, such as the flow field characteristics of the geometry system, the rheological characteristics, and the mixing behavior of the fluids. There are several computational studies on influential parametric in the mixing process i.e., an impeller layout (Rahimi, 2005), impeller rotational speed, position and flow rate of the feed (Zhang et al., 2009), working fluid rheology (Wu, 2011),

* Corresponding author.
E-mail address: widodo@che.ui.ac.id (W.W. Purwanto).

https://doi.org/10.1016/j.egyr.2019.04.008

various impeller and working fluid rheology (Sossa-Echeverria and Taghipour, 2015), and propeller layout and working fluid rheology (Wiedeman et al., 2018).

Molasses is a bioethanol production feedstock that contains non-sugar ingredients such as organic acids, lipids and inorganic salts, and macromolecules; these constituents affect the inherently high viscosity of molasses (Kaur et al., 2002). A viscous fluid tends to exhibit non-Newtonian behavior; for that reason, the influence of the rheological parameters cannot be ignored in the mixing system (Oropeza-De la Rosa et al., 2017). The research related to non-Newtonian fluid mixing includes the mixing to a pseudoplastic fluid (Wiedemann et al., 2017; Conti et al., 2018), a yield-pseudoplastic fluid (Jegatheeswaran et al., 2017) and a viscoelastic fluid (Ramsay et al., 2016b,a). Furthermore, the rheological properties of molasses are affected by the shear rate, which is in turn strongly influenced by the temperature and concentration of molasses in the mixture. Several studies have been conducted to study the effect of the addition of ethanol (Toğrul and Arslan, 2004), dextran (Oropeza-De la Rosa et al., 2017), and starch (Kaur et al., 2002) on the rheological properties of molasses. The mixing of a highly viscous molasses fluid leads to flow in the tangential direction that is generated by the impeller; as a result, fluid flows were limited to the region near the impeller (Gómez et al., 2010). Consequently, it necessary to dilute molasses by adding water to obtain the suitable conditions for the yeast. Therefore, it is essential to investigate the effect of water content on the rheological characteristics of molasses in order to determine the right conditions for the fermentation process.

This research is a continuation of the previous research that reviewed the effectiveness of mixing of different propeller installments (Madhania et al., 2017) and the mixing phenomena are observed for the different computational solution strategies (Madhania et al., 2018). However, in the previous work, the rheological factor was neglected. Thus, in this work, we will experimentally study the molasses–water mixing behavior inside a stirred vessel by simple visualization method include rheology characteristic and computationally study in revealing the turbulence phenomena through CFD.

2. Methods

Experiments were carried out to obtain the rheological characteristics of pure molasses and molasses–water mixture, also the mixing behavior of molasses–water in a stirred tank. Then, computational modeling was performed to reveal the fluid dynamics of the molasses–water mixing under turbulent conditions. The modeling was carried out by using the commercial code of ANSYS Fluent version 18.2.

2.1. Experimental

The experiments were divided into two steps. The first step was to characterize the rheological properties of pure molasses and molasses–water mixture. The second step was to analyze the mixing behavior based on the data obtained by using a visualization method.

2.1.1. Rheological characterization

The rheological characterization was carried out on two types of molasses, referred to as type-A and type-B, where type-A seem more viscous than type-B. An experiment was conducted by using a Brookfield rheometer to investigate the rheological characteristics such as shear stress, shear rate, also apparent viscosity of the molasses and obtain a quantitative difference between each sample, especially since it is possible that both samples represent a non-Newtonian fluid. The viscosity of the pure molasses was measured.

$$\tau = K\dot{\gamma}^n \tag{1}$$

Where τ is the shear stress (Pa), K is the consistency index (Pa s^n), and $\dot{\gamma}$ is the shear rate (s^{-1}).

2.1.2. Mixing behavior

The mixing of molasses and water was carried out by using a half-cylindrical, half-coned stirred-tank. The tank has a cylindrical geometry for the upper part and is cone-shaped in the lower part. A propeller is located in the cone part and is positioned perpendicular to its surface, as can be seen in Fig. 1a. This tank was filled with molasses up to a height of 0.155 m in the cylinder part, and tap water was carefully filled from this side. The three-bladed propeller was then rotated at the velocities of 1000 rpm, 1100 rpm, 1200 rpm, and 1300 rpm. A tachometer was used to ensure the accuracy of the rotational speed of the propeller.

A simple visualization experiment based on a coloring /decoloring method (Conti et al., 2019) by using a high speed camera as seen in Fig. 1(b). A camera is positioned in front of the tank to record the change in the height of the interface that separates the molasses and water during the entire mixing process, which is indicative of the mixing behavior. In order to add contrast between the molasses and the water, a red laser of wavelength 650 nm was used to illuminate the fluid inside. The use of a laser as an observation plane is adopted by the PIV principle, to observe changes in interface height between two fluids.

The images were then processed by data acquisition by using an image processing technique to obtain the location of the interface. The sequence of image processing is shown in Fig. 2.

2.2. Computational

The turbulent phenomena related to the mixing process of molasses and water are based on the turbulent flow regime that is observed during the mixing experiment. This phenomenon was modeled computationally by applying the commercial code ANSYS Fluent 18.2. The calculations were performed in 3D and transient. This research involved two studies; the first was the determination of an appropriate multiphase model of molasses–water mixing based on the experimental scale while the second in an industrial-scale fermenter. The dimensions of these two studies are summarized in Table 1.

The geometry of the computational domains was generated by the ANSYS design modeler, and the flow domain was divided into tetrahedral meshes by using ANSYS, as shown in Fig. 3. This geometrical models are similar with mesh models and its stirred vessel comprised of static zone and moving zone as the previous study (Wiedeman et al., 2018).

Table 1
Dimensions of the computational domains and grid-generation information.

		Small scale	Industrial scale
Geometry	Tank diameter (m)	0.28	7
	Tank height (m)	0.395	9.87
	Propeller diameter (m)	0.036	0.9
Meshing	Nodes :		
	- Static zone	26 734	134 161
	- Moving zone	132 437	127 184
	Element :		
	- Static zone	112 848	713 610
	- Moving zone	536 719	689 081
	Average dimension	0.25	0.83

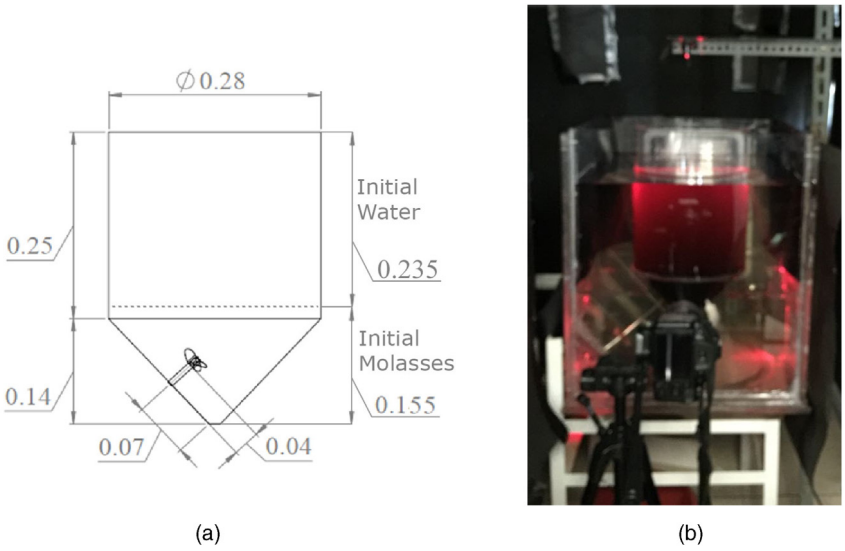

Fig. 1. Dimensions of the system (a) and the experimental setup (b).

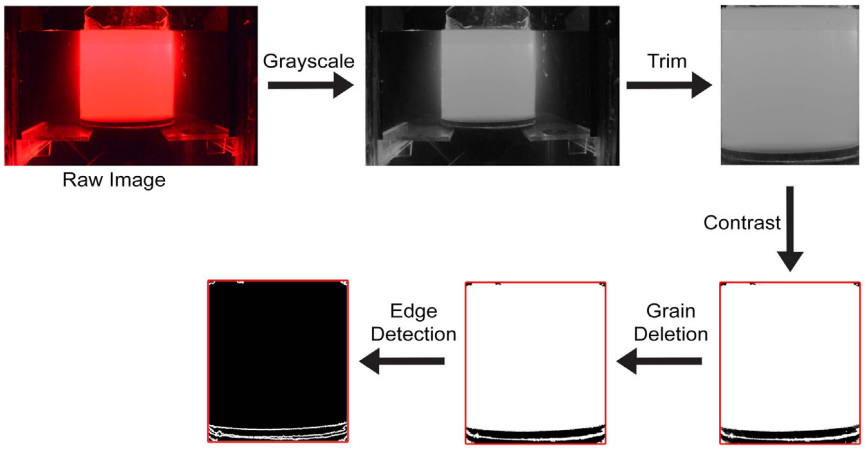

Fig. 2. The sequence of image processing.

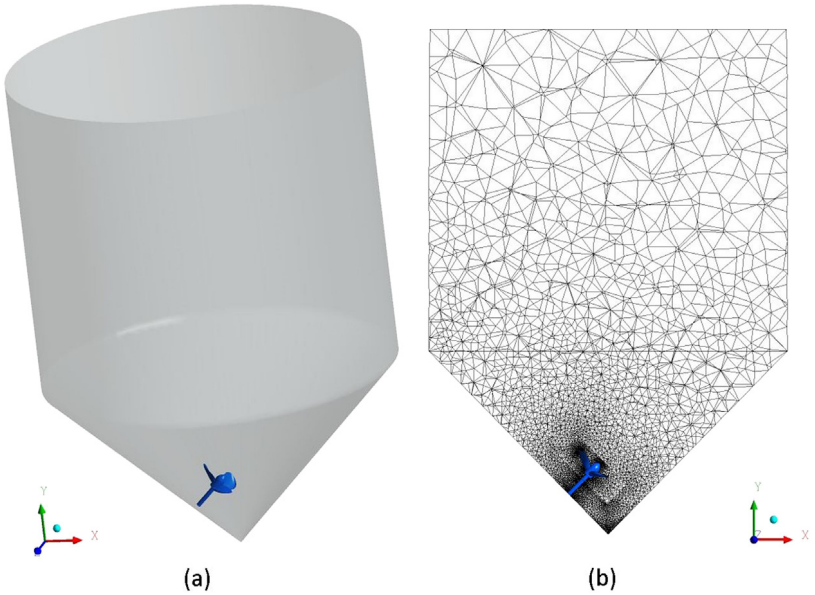

Fig. 3. The computational domain (a) and grid generation (b).

Table 2
Rheological characteristics of molasses.

	Type-A	Type-B
K	11 017	1320.3
n	0.9057	0.9364
R^2	0.9726	0.9933

The working fluids consist of molasses and water, which are mutually dissolved with the viscosities of 0.001003 Pa.s for water and 0.076044 Pa. s for molasses. The initial mass fraction of water–molasses in the liquid system is defined relative to their heights in the vessel. The height of the molasses inside the vessel was set at 0.155 m, and the height of the water that fills the vessel was set at 0.235 m above the molasses. Two distinct layers are formed because of the difference in density.

The stirred vessel comprised two parts: a moving zone around the impeller and a stationary zone which attached to the vessel wall. The interface between a moving zone and a stationary zone was treated as an interface boundary condition. The shaft can be regarded as an absolute moving wall. The propeller was set to the moving wall, which was relative to the moving zone. The model describes the turbulence phenomenon that observed at the propeller rotational speed of 1300 rpm; thus, the velocity of the moving zone and shaft were set to the angular velocity ($N = 1300$ rpm). This study applied Large Eddy Simulation (LES) to model the turbulent flow as based on previous work (Madhania et al., 2018). The Mixture and the Eulerian model were applied to represent the multiphase flow. At the liquid surface, the axial gradient of the dependent variables was set to zero (symmetry boundary condition). The conical bottom and cylindrical walls were those derived by assuming non-slip conditions and were treated as stationary walls. No-slip implies that the velocity of the fluid at the wall boundary is zero.

The operating conditions were defined by considering gravity along the y-axis ($g = -9.81$ m/s^2) and setting the unit of the angular speed to rotations per minute. Coupling between the continuity and momentum equations was achieved by using Semi-Implicit Method for Pressure-Linked Equations (SIMPLE) (Van Doormaal and Raithby, 1984). The spatial discretization was set to first-order upwind for the momentum, volume fraction, turbulent kinetic energy, and turbulent dissipation rate equations (Ansys-Fluent, 2013). The Pressure Staggering Option (PRESTO) was used for the spatial discretization of pressure (Bender, 1981). The convergence criterion was set to 1×10^{-5} for the velocities and 1×10^{-4} for the volume fractions. The first-order implicit scheme was used for the time step of the turbulence model. The time step was set to 0.001 s. The under-relaxation factors of the numerical scheme were initially set to 0.3 for pressure, 0.5 for momentum, and 0.5 for volume fraction.

3. Results and discussion

3.1. Rheological properties

The rheological properties were characterized in terms of the shear stress and shear rate data. The shear rate versus shear stress relationships representing the rheograms of the different molasses samples are shown in Fig. 4.

As depicted in the rheogram, disproportionality between the shear stress and the shear rate is observed for both the molasses types, which indicates non-Newtonian fluid behavior. The type-A molasses requires higher shear stress to flow than the type-B molasses. The rheological characteristics of both the molasses types are shown in Table 2.

Based on Table 2, the flow curves were well fitted to the power law model with n < 1 was obtained. It can be concluded that

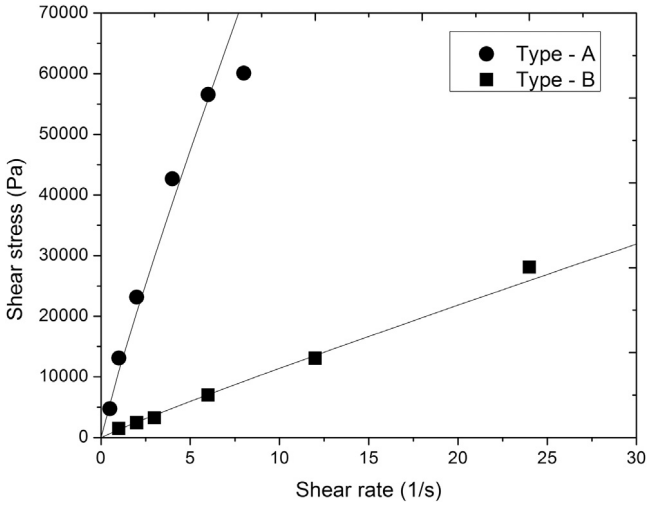

Fig. 4. Rheological behaviors of pure molasses.

both of the samples belong to the category of shear thinning or pseudoplastic fluids, which is in accordance with a study of Oropeza-De la Rosa et al. (2017).

As for type-B, it also reveals the shear thinning fluid behavior, though it is much less significant because it decreases only in a small range of shear rates before stabilizing at the observed value. As such, it is possible to consider type-B as a Newtonian fluid, but, in this case, we would still consider it as a shear thinning fluid.

The apparent viscosity profile is shown in Fig. 5. It is observed that for both the samples, even though the viscosity decreases with time, it stabilizes relatively quickly. The viscosity decreases with an increase in the shear rate, and this relation is much more apparent in the type-A molasses. This is because the long chains of molecules disentangle with an increase in the shear rate so that the intermolecular resistance to flow becomes smaller (Toğrul and Arslan, 2004). However, the most significant change is observed upon the addition of water. Even a small amount of water in the molasses could drastically reduce its viscosity. Owing to the water molecules that position themselves between the molasses molecules, the molecular attractions can substantially change, which in turn reduce the viscosity. This effect is observed in both types of molasses.

The existing mathematical models which used to calculate for non-Newtonian fluid are include the power law model, Cross model (Cross, 1965), and Carreau model (Akbar and Nadeem, 2014; Yasuda, 2005; Carreau, 1972). There are current studies on the effect of temperature and concentration of the ethanol added (Toğrul and Arslan, 2004) and presence of starch (Kaur et al., 2002) on the apparent viscosity of molasses, however there is no model has been yet developed that calculates both the variables of shear rate (γ) and the amount of water added (χ) simultaneously. As a result, a new apparent viscosity model of the molasses–water mixture was developed empirically ($R^2 = 0.9962$ for type-A molasses and 0.9977 for type-B molasses) for predicting with both the variables as follows:

$$\mu_A = \left(2000e^{-28.5\chi+1.305} + 150.12 - 148\chi^{3.5}\right) \times \left(1.46e^{-0.125\gamma} + 0.4666\right) \quad (2)$$

$$\mu_B = \left(378e^{-17.5\chi+1.05} + 45 - 44\chi^{20}\right)\left(1.47e^{-1.51\gamma} + 1\right) \quad (3)$$

3.2. Mixing behavior

As the interface would rise as the molasses is mixed with water, it reveals how the molasses molecules move or mix with

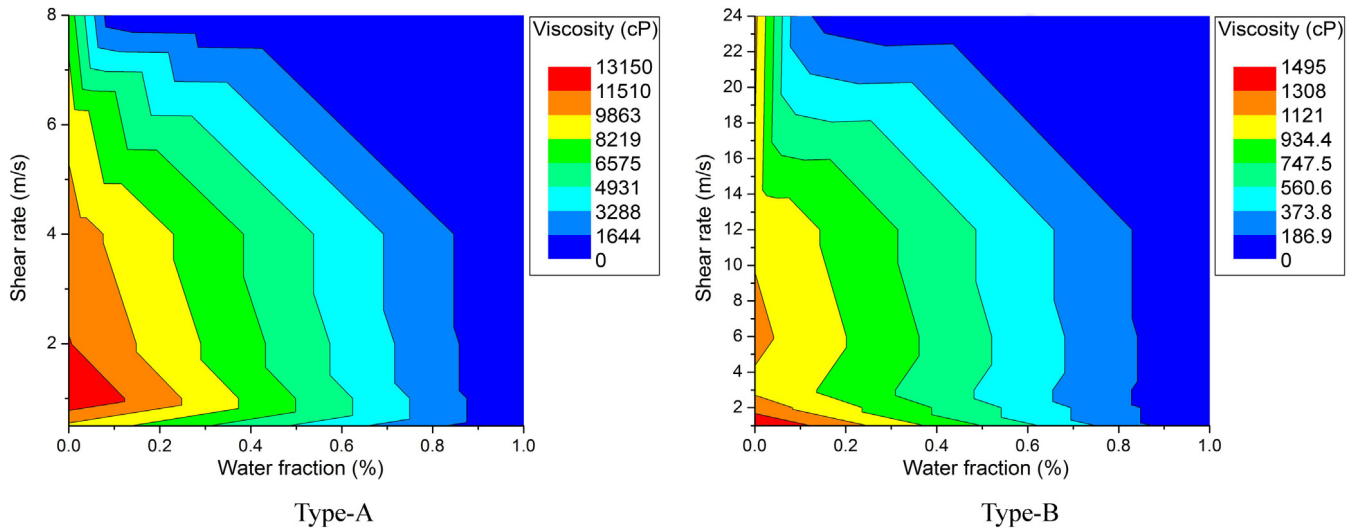

Fig. 5. Type-A and type-B molasses.

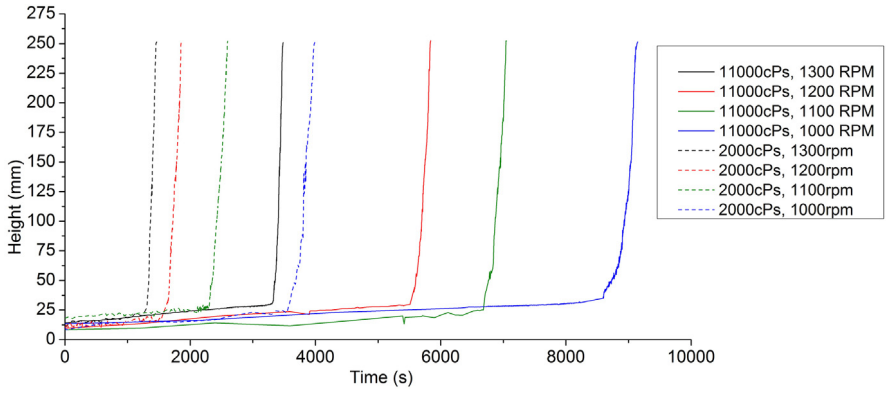

Fig. 6. Mixing behavior of molasses–water as functions of time for different propeller rotation speeds for both type-A and type-B molasses.

the water. The changes in the interface height during the entire mixing process can be seen in Fig. 6.

Based on visual observations, the proposed mechanism of the molasses–water mixing process comprises three different zones as can be seen in Fig. 7. In zone one, the height of the interface is slightly increasing in the short period corresponds to the propeller which has just started to rotate. As the propeller spins, the molasses that are in direct contact with it get sucked into the negative-axial direction toward to propeller. This phenomenon happens due to the propeller lost its pumping ability because of the high of molasses viscosity level. The energy shifted by the propeller, initially reach only the molasses at the blade tip. The longer of the stirring process, the effect of propeller rotation become wider until it reaches the interface area causes water sucked in and penetrate the interface boundary then move following the direction of the flow pattern generated by the propeller rotation. As the region where the sucked-up molasses usually resides is then occupied by water, the molasses would need some other place to occupy, which leads to an increase in the interface height.

Zone two phenomena are similar to zone one. However, the interface height changes occur slowly over a long period because of the ability of the propeller to distribute water in the molasses-rich regions that were influenced by the mixture rheology, especially viscosity. Based on the rheological characterization, upon adding a small amount of water, the viscosity of the mixture is significantly less than the viscosity of the pure molasses. The effect of changes in properties of fluid mixture around the propeller very affected on its pumping capacity. This mixing process requires a long time to reach a viscosity that equals to 0.007604 Pa; then in this condition, the propeller has a pumping ability in order to push the fluid outwards. At some points, on the surface of interface occurs turbulence condition that leads fluid to enter zone three.

Zone three is where most of the mixing process occurs. Though this zone is observed only for the final 6%–12% of the total mixing time, it accounts for more than 90% of the mixing process. This zone observed when the interface height increase occurs rapidly as can be seen in Fig. 8. A similar study to estimate the mixing characteristic has been reported by Conti et al. (2019).

3.3. Turbulence phenomena

The predicted phenomena for the mixing of molasses and water under the turbulence regime of zone three as generated by different multiphase models are analyzed by the height of interface changes in every time on density contour which has shown in Fig. 8 and being compared to the mixing behavior that observed experimentally. It can be seen that the phenomenon

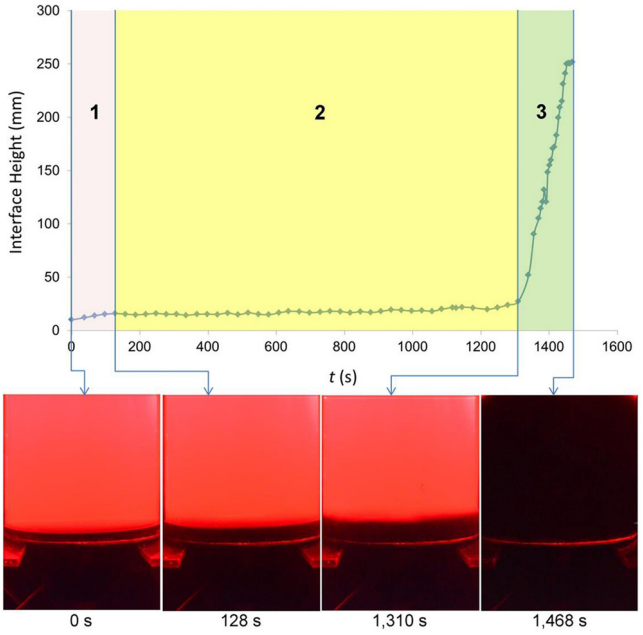

Fig. 7. The photograph of the mechanism for the molasses–water mixing process of type-B molasses at 1300 rpm.

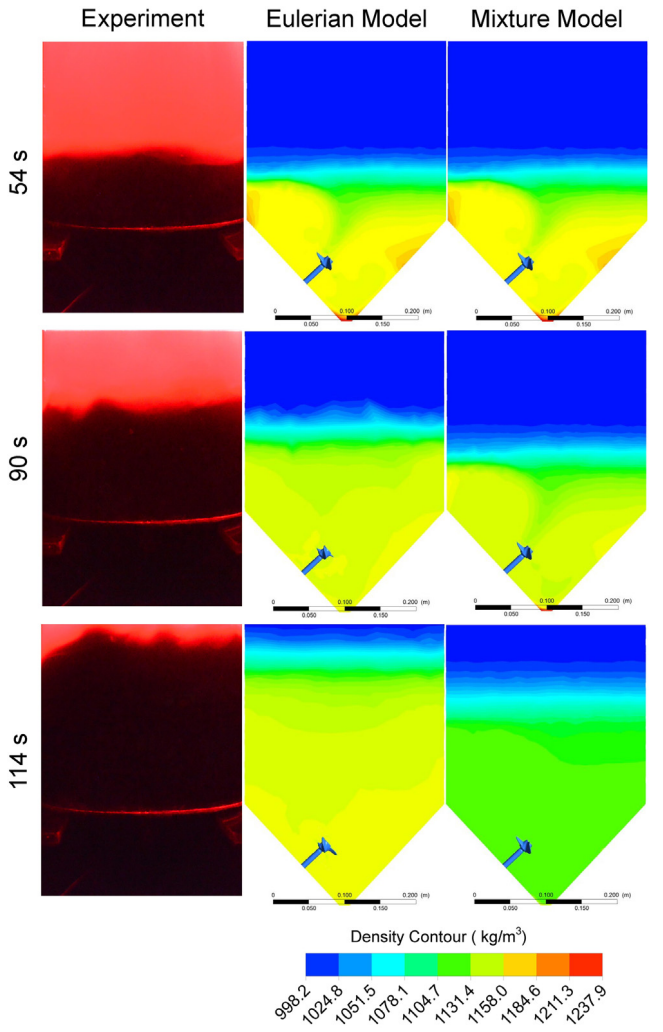

Fig. 9. Comparison of the changes in the height of the interface observed experimentally and those predicted by computations generated by the Mixture and Eulerian multiphase model at zone three.

resulting from the Eulerian approach is the closest to the experimental results. It suggests that zone three phenomena are most precisely modeled by using the Eulerian approach (see Fig. 9).

The Eulerian multiphase model was then used to model the molasses–water mixing phenomena for industrial-scale stirred tanks and predict the time to reach a homogeneous condition, as shown in Fig. 10. Based on an analysis of the changes in the density of the mixture at a point, the mixing time to reach a homogeneous condition was obtained as 114 s.

The homogeneous conditions can also be viewed in terms of the changes in the density in the vertical plane of observation (plane-XY), as shown in Fig. 11, and in the horizontal plane of observation (plane-XZ), shown in Fig. 12. Based on these two images, the changes in the density contours over time reveal that the process occurs from the start of stirring until a homogeneous condition is reached. The contour change can also describe the turbulence observed in the stirred tank. As can be seen in the final mixing condition, there is no dead zone; hence, the degree of mixing is 0.998992.

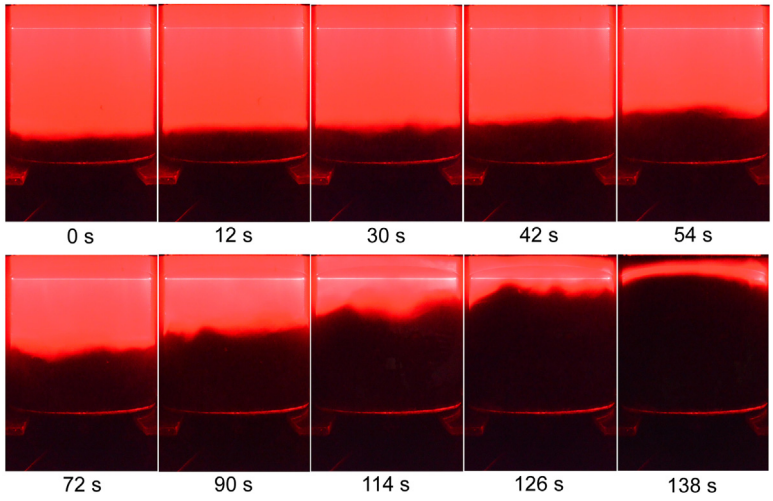

Fig. 8. Mixing behavior of molasses–water for type-A molasses at 1300 rpm in zone three.

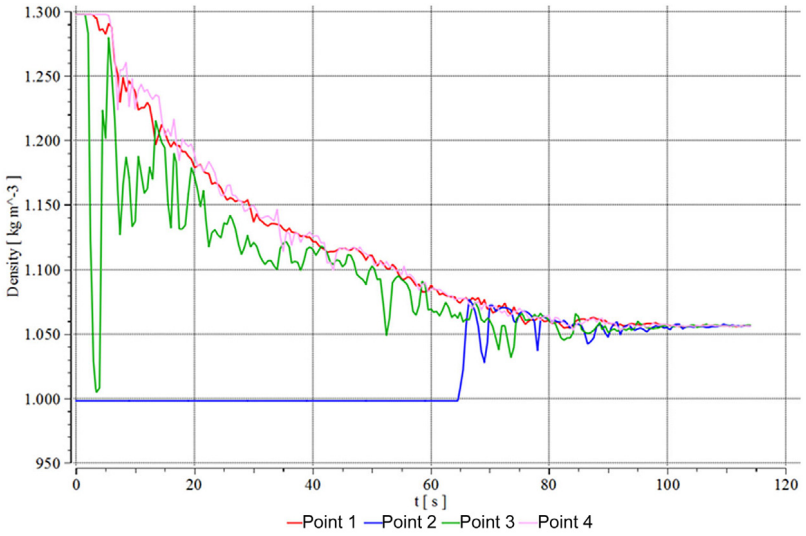

Fig. 10. Time to achieve homogenization in the mixing of molasses and water.

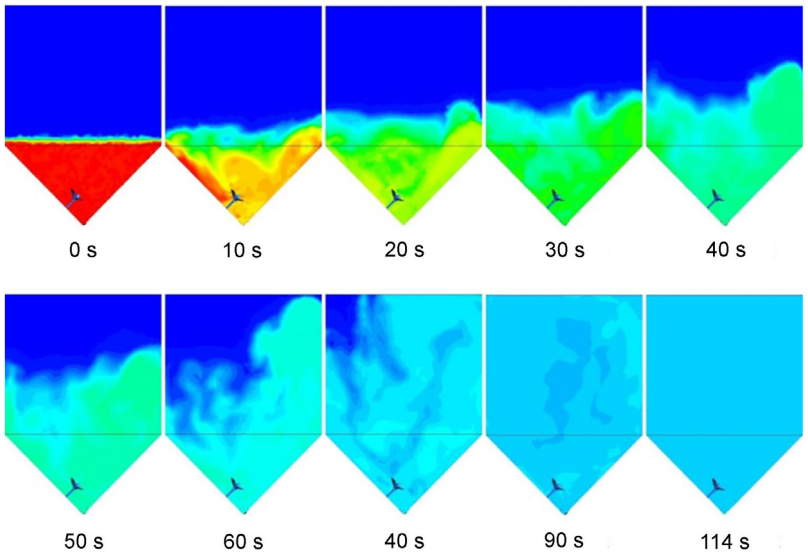

Fig. 11. Changes in density contour on the *XY*-plane (*plane-z*).

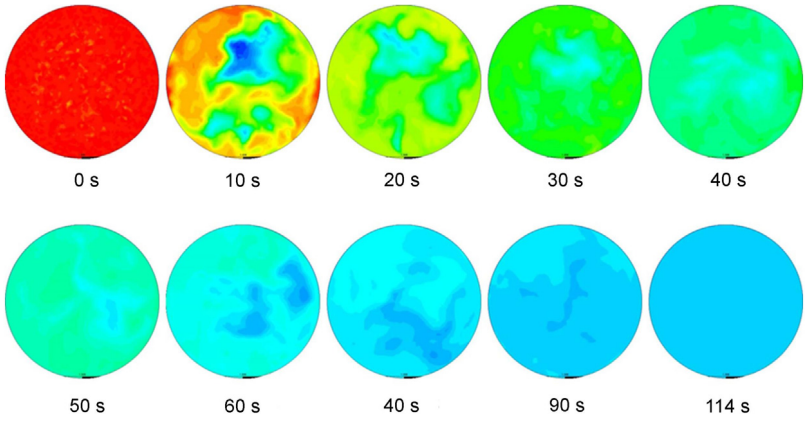

Fig. 12. Changes in density contour on the *XZ*-plane (*plane-y*).

4. Conclusion

Mathematical models were developed for predicting the apparent viscosity of molasses based on experimental of rheology characterization both the variables of shear rate and molasses–water ratio. Molasses–water mixture showed shear thinning behavior.

The mixing behavior experimental results showed that molasses–water mixture comprised into three zone mechanisms which the rheological properties and propeller rotation speed are the most influential factors.

The simulation revealed that the Eulerian multiphase model is a model that closest to the experimental results at zone three. Moreover, the combination of the Eulerian multiphase model and Large Eddy Simulation can be applied to predict the mixing behavior in industrial scale stirred tank.

Acknowledgments

This work has been carried out with the financial support of Universitas Indonesia under the project "Hibah Tugas Akhir Doktor" 2018 (contract number: 1367/UN2.R3.1/HKP.05.00/2018).

References

Akbar, N.S., Nadeem, S., 2014. CaRreau fluid model for blood flow through a tapered artery with a stenosis. Ain Shams Eng. J. 5, 1307–1316.
Ansys-Fluent, 2013. Fluent 15.0 Documentation Fluent Theory Guide. Canonsburg, P.A., USA, ANSYS, Inc.
Bender, E., 1981. Numerical heat transfer and fluid flow. Von S. V. Patankar. Hemisphere Publishing Corporation, Washington – New York – London, McGraw Hill Book Company, New York 1980 1 Aufl., 197 S., 76 Abb., geb., DM 71, 90 Chem Ing Tech, 53, 225-225.
Bibi, R., Ahmad, Z., Imran, M., Hussain, S., Ditta, A., Mahmood, S., Khalid, A., 2017. Algal bioethanol production technology: A trend towards sustainable development. Renew. Sust Energy Rev. 71, 976–985.
Boonchuay, P., Techapun, C., Leksawasdi, N., Seesuriyachan, P., Hanmoungjai, P., Watanabe, M., Takenaka, S., Chaiyaso, T., 2018. An integrated process for xylooligosaccharide and bioethanol production from corncob. Bioresour. Technol. 256, 399–407.
Byadgi, S.A., Kalburgi, P.B., 2016. Production of bioethanol from waste newspaper. Procedia Environ. Sci. 35, 555–562.
Carreau, P., 1972. Rheological Equations from Molecular Network Theories.
de Carvalho, A.L., Antunes, C.H., Freire, F., 2016. Economic-energy-environment analysis of prospective sugarcane bioethanol production in Brazil. Appl. Energy 181, 514–526.
Chao, B., Liu, R., Zhang, X., Zhang, X., Tan, T., 2017. Tannin extraction pretreatment and very high gravity fermentation of acorn starch for bioethanol production. Bioresour. Technol. 241, 900–907.
Conti, F., Wiedemann, L., Sonnleitner, M., Saidi, A., Goldbrunner, M., 2018. Thermal behavior of viscosity of aqueous cellulose solutions to emulate biomass in anaerobic digesters. New J. Chem. 42, 1099–1104.
Conti, F., Wiedemann, L., Sonnleitnmer, M., Saidi, A., Goldbrunner, M., 2019. Monitoring the mixing of an artificial model substrate in a scale-down laboratory digester. Renew. Energy 132, 351–362.
Cross, M.M., 1965. Rheology of non-Newtonian fluids: A new flow equation for pseudoplastic systems. J. Colloid Interface Sci. 20, 417–437.
Gómez, C., Bennington, C.P.J., Taghipour, F., 2010. Investigation of the flow field in a rectangular vessel equipped with a side-entering agitator. J. Fluid Eng. 132, 051106–051106–13.
Jegatheeswaran, S., Ein-Mozaffari, F., Wu, J., 2017. Efficient mixing of yield-pseudoplastic fluids at low reynolds numbers in the chaotic SMX static mixer. Chem. Eng. J. 317, 215–231.
Kaur, S., Kaler, R.S.S., Aamarpali, 2002. Effect of starch on the rheology of molasses. Int. J. Food Eng. 55, 319–322.
Khambhaty, Y., Mody, K., Gandhi, M.R., Thampy, S., Maiti, P., Brahmbhatt, H., Eswaran, K., Ghosh, P.K., 2012. Kappaphycus alvarezii as a source of bioethanol. Bioresour. Technol. 103, 180–185.
Liu, Y.-K., Chen, W.-C., Huang, Y.-C., Chang, Y.-K., Chu, I.M., Tsai, S.-L., Wei, Y.-H., 2017. Production of bioethanol from napier grass via simultaneous saccharification and co-fermentation in a modified bioreactor. J. Biosci. Bioeng. 124, 184–188.
Madhania, S., Cahyani, A.B., Nurtono, T., Muharam, Y., Winardi, S., Purwanto, W.W., 2018. CFD Study of mixing miscible liquid with high viscosity difference in a stirred tank. IOP Conf. Ser.: Mater. Sci. Eng. 316, 012014.
Madhania, S., Nurtono, T., Cahyani, A.B., Carolina, Muharam, Y., Winardi, S., Purwanto, W.W., 2017. Mixing behaviour of miscible liquid-liquid multiphase flow in stirred tank with different marine propeller installment by computational fluid dynamics method. Chem. Eng. Trans. 56, 1057–1062.
Mohd Azhar, S.H., Abdulla, R., Jambo, S.A., Marbawi, H., Gansau, J.A., Mohd Faik, A.A., Rodrigues, K.F., 2017. Yeasts in sustainable bioethanol production: A review. Biochem. Biophys. Rep. 10, 52–61.
Rahimi, M., 2005. The effect of impellers layout on mixing time in a large-scale crude oil storage tank. J. Pet. Sci. Eng. 46, 161–170.
Ramsay, J., Simmons, M.J.H., Ingram, A., Stitt, E.H., 2016a. Mixing of Newtonian and viscoelastic fluids using butterfly impellers. Chem. Eng. Sci. 139, 125–141.
Ramsay, J., Simmons, M.J.H., Ingram, A., Stitt, E.H., 2016b. Mixing performance of viscoelastic fluids in a kenics KM in-line static mixer. Chem. Eng. Res. Des. 115, 310–324.
Oropeza-De la Rosa, E., López-ávila, L.G., Luna-Solano, G., Cantú-Lozano, D., 2017. Bioethanol production process rheology. Ind. Crop Prod. 106, 59–64.
Virgínio e Silva, J.O., Almeida, M.F., Da Conceição Alvim-Ferraz, M., Dias, J.M., 2017. Integrated production of biodiesel and bioethanol from sweet potato. Renew. Energy.
Sossa-Echeverria, J., Taghipour, F., 2015. Computational simulation of mixing flow of shear thinning non-Newtonian fluids with various impellers in a stirred tank. Chem. Eng. Process.: Process. Intensification 93, 66–78.
Tgarguifa, A., Abderafi, S., Bounahmidi, T., 2017. Modeling and optimization of distillation to produce bioethanol. Energy Procedia 139, 43–48.
Tomás-Pejó, E., Oliva, J.M., González, A., Ballesteros, I., Ballesteros, M., 2009. Bioethanol production from wheat straw by the thermotolerant yeast kluyveromyces marxianus CECT 10875 in a simultaneous saccharification and fermentation fed-batch process. Fuel 88, 2142–2147.
Toğrul, H., Arslan, N., 2004. Mathematical model for prediction of apparent viscosity of molasses. J. Food Eng. 62, 281–289.
Van Doormaal, J.P., Raithby, G.D., 1984. Enhancements OF THE SIMPLE method FOR predicting incompressible FLUID flows. Numer. Heat Transfer 7, 147–163.
Wang, L., Sharifzadeh, M., Templer, R., Murphy, R.J., 2012. Bioethanol production from various waste papers: Economic feasibility and sensitivity analysis. Appl. Energy 117, 2–1182.
Wiedeman, L., Conti, F., Saidi, A., Sonnleitner, M., Goldbrunner, M., 2018. Modeling mixing in anaerobic digesters with computational fluid dynamics validated by experiments. Chem. Eng. Technol. 41, 2101–2110.
Wiedemann, L., Conti, F., Janus, T., Sonnleitner, M., Zörner, W., Goldbrunner, M., 2017. Mixing in biogas digesters and development of an artificial substrate for laboratory-scale mixing optimization. Chem. Eng. Technol. 40, 238–247.
Wu, B., 2011. CFD Investigation of turbulence models for mechanical agitation of non-Newtonian fluids in anaerobic digesters. Water Res. 45, 2082–2094.
Yasuda, K., 2005. Investigation of the analogies between viscometric and linear viscoelastic properties of polystyrene fluids.
Zhang, Q., Yong, Y., Mao, Z.S., Yang, C., Zhao, C., 2009. Experimental determination and numerical simulation of mixing time in a gas–liquid stirred tank. Chem. Eng. Sci. 64, 2926–2933.